



N₂ Chemistry in Interstellar and Planetary Ices: Radiation-driven Oxidation

Reggie L. Hudson

Astrochemistry Laboratory, NASA Goddard Space Flight Center, Greenbelt, MD 20771, USA; Reggie.Hudson@NASA.gov*Received 2018 May 27; revised 2018 September 25; accepted 2018 September 29; published 2018 November 12*

Abstract

As part of our work on nitrogen-rich ices, the IR spectra and band strengths used in a recent paper to identify and quantify radiation-induced changes in an N₂+H₂O ice near 15 K are examined, along with reports of (i) a chemical tracer for N₂+H₂O ices, (ii) a new IR feature of solid N₂, and (iii) a striking ¹⁵N isotopic enrichment. Problems are found for each IR band strength used and for each of the three claims made, to the extent that none are supported by the results presented to date. In contrast, new work presented here, combined with several older investigations, strongly supports the formation of di- and triatomic nitrogen oxides in irradiated N₂-rich ices. Observations and trends in the chemistry of N₂-rich icy solids are described, and conclusions are drawn. A considerable amount of material from previous chemical studies of N₂-rich systems, spanning more than a century, is brought together for the first time and used to examine the chemistry of N₂-rich ices in extraterrestrial environments. Needs are identified and suggestions made for future studies of N₂-rich interstellar and planetary ice analogs.

Key words: astrobiology – astrochemistry – infrared: ISM – ISM: molecules – molecular data

1. Introduction

The use of laboratory methods to study the chemistry of ices in the interstellar medium (ISM) and the outer solar system is well established and supported by an extensive set of publications. In our laboratory group, we have focused on reaction chemistry applicable to extraterrestrial ices and on the application of standard spectroscopic methods to identify and quantify the many solid-phase molecules and ions of astronomical interest. However, the diversity of icy solids and the range of astronomical environments make it unrealistic and tedious to attempt to examine all possible combinations of temperature, composition, molecular type, radiation doses, and radiation forms in terrestrial laboratories, and so it is imperative to seek patterns and trends in the chemistry of icy materials. As an example, some years ago we examined radiation-chemical reactions in cometary and interstellar ice analogs, showing how unsaturated compounds could be reduced to their saturated counterparts by solid-state radiolysis, such as the conversion of C₂H₂ into C₂H₆ (Hudson & Moore 1997) and CO into CH₃OH (Hudson & Moore 1999). More recently we have turned to radiation-driven oxidations, such as the conversion of solid propene into propylene oxide (Hudson et al. 2017b), which has been detected in the ISM (McGuire et al. 2016), and the low-temperature synthesis of aldehydes and ketones from alcohol-containing ices (Hudson & Moore 2018).

Background information on the radiation chemistry of icy solids is available in many earlier papers from our research group (e.g., Moore 1999; Hudson et al. 2001), from publications by other workers (e.g., Strazzulla 1998; Bennett et al. 2007, 2013), and from the many references therein, and so only a summary is given here. Cosmic radiation, magnetospheric radiation around planets, and stellar (including solar) far-UV photons and solar energetic particles all act to drive chemical reactions at low temperatures. In the case of cosmic and other magnetospheric radiation (particle radiations), the dominant components are hydrogen and helium ions. As each ion passes through an icy solid, it produces a track of ionizations and excitations. The ionizations generate secondary electrons that can continue to generate chemical change

through a variety of reactions. In all cases, the initial ion's energy will be degraded and, in ices that are sufficiently thick, the ion will be trapped (thermalized) and implanted at the end of its trail. It is important to appreciate that the chemical products made by various radiations acting on extraterrestrial ices are largely the result of secondary electrons and that while reaction yields and spatial distributions of products can vary, the identities of those reaction products are expected to be largely the same across a wide variety of radiation types and energies. This makes it difficult, if not impossible, to distinguish among ices that have been irradiated by, for example, keV e⁻, X-, and γ -rays and MeV H⁺, He⁺, and higher-mass ions.

Although most of our laboratory work on astronomical ices and radiation chemistry has focused on solids rich in highly polar molecules, such as H₂O, H₂O₂, alcohols, and nitriles, some astronomical ices are dominated by nonpolar molecules. Specifically, Triton, Pluto, and Eris have surface ices rich in N₂ (Cruikshank et al. 1984; Owen et al. 1993; Tegler et al. 2012), and ice mantles on interstellar grains are thought to have regions that are deficient in H₂O ice and rich in nonpolar (or weakly polar) species, such as N₂, O₂, and CO (Ehrenfreund et al. 1998; Rosu-Finsen et al. 2016). Our earlier work with such solids examined proton-irradiated N₂+CH₄ and N₂+CH₄+CO ices to demonstrate the formation of both HCN and HNC (Moore & Hudson 2003). This soon was followed by a study of several organic nitriles in solid N₂ to demonstrate production of ketenimine (Hudson & Moore 2004), which subsequently was found in the ISM (Lovas et al. 2006). However, oxidation in nitrogen-rich ices has received relatively little attention, and so we recently have examined such reactions for applications to N₂-containing interstellar ices and to outer solar system bodies, such as trans-Neptunian objects (TNOs).

One example of the use of ionizing radiation to study N₂-rich ices, from a laboratory other than ours, is the work of de Barros et al. (2015) on the chemical changes produced by irradiating N₂+H₂O ice at 15 K with 40 MeV ⁵⁸Ni¹¹⁺. However, while comparing our work to that study, which we abbreviate as dB15, we encountered a large number of questionable items,

about a dozen of which are described in our Appendix A. Instead of addressing each of them and trying to determine which are typographical errors and which are not, here we focus on the assignments of IR bands of reaction products reported by dB15 and on three claims in that paper that are, if valid, of considerable astrochemical significance. Note that the generation of a large amount of new numerical information based on reference data of questionable relevance or accuracy is specifically avoided. A primary goal is to extract results from dB15 that can be combined with published work from several laboratories, including new results presented here, to uncover some points of commonality in studies of radiolytic oxidation in N₂-rich icy solids and to identify some areas where new work is needed. A strong emphasis is placed on using a variety of spectroscopic methods to firmly assign reaction products since without robust spectral assignments it will be difficult to move forward in our understanding of the chemistry of N₂-rich ices.

2. Laboratory Methods

The laboratory work for this paper used in situ mid-IR spectroscopy to reveal chemical and physical changes in icy solids irradiated near 15 K by a 1 MeV H⁺ beam. Ices were grown on a pre-cooled aluminum or gold substrate inside a vacuum chamber interfaced to a Van de Graaff accelerator, the source of the proton beam (current $\sim 0.1 \mu\text{A}$). An IR spectrum of the sample was collected by reflecting the IR beam off the sample and underlying substrate (range = 5000–650 cm⁻¹, resolution = 0.5 cm⁻¹, 100 scans per spectrum). See our group's recent papers and references therein for details of our spectroscopic, cryogenic, vacuum, and radiation equipment (e.g., Hudson et al. 2017a; Hudson & Moore 2018). In all cases, ice thicknesses were smaller than the range of the incident radiation beam ($\sim 33 \mu\text{m}$), ensuring irradiation throughout each ice sample. As in the past, the use of band strengths to determine the thickness of each of our ices has been avoided in favor of the method of interference fringes as a more direct measurement (e.g., Tempelmeyer & Mills 1968; Hudson et al. 2017a). The index of refraction of our N₂-rich ices was taken as $n = 1.22$ (Satorre et al. 2008). Sigma Aldrich (USA) was the source of all reagents used, including those that were isotopically enriched.

To support our work, the electronic stopping power (S_{el}) of solid N₂ was calculated with the SRIM package of Ziegler et al. (1985; 2013 version), using a density of $\rho(\text{N}_2) = 0.94 \text{ g cm}^{-3}$ (Satorre et al. 2008) and a compound correction of 1 (Ziegler & Manoyan 1988). The results are, to two significant figures, $S_{\text{el}} = 20 \text{ keV } \mu\text{m}^{-1}$ for 1 MeV H⁺ and $S_{\text{el}} = 3600 \text{ keV } \mu\text{m}^{-1}$ for the 40 MeV ⁵⁸Ni¹¹⁺ of de Barros et al. (2015). The dose in eV molecule⁻¹ received by an ice is found from the product “ $mS_{\text{el}}F$,” where m is the mass of a sample molecule (or average mass), S_{el} is the sample's electronic stopping power, and F is the fluence of incident ions on the sample, typically with units of ions cm⁻². This means that an incident proton fluence of $1.0 \times 10^{14} \text{ H}^+ \text{ cm}^{-2}$ on our ices, all of which are N₂ rich, is equivalent to an absorbed dose of about 3.37 MGy, 337 Mrad, and 0.98 eV per N₂ molecule. Nuclear stopping powers are about 0.1% of S_{el} for our ices and so are ignored.

3. Results

Before presenting new data from our own laboratory, we first consider some results from the paper of de Barros et al. (2015) that concern the identification and quantification of reactants and products in the irradiation of an N₂-rich ice sample. We show that significant questions accompany some of the results described there. However, and more positively, we also show that there are important common points between other results in that paper, some findings in other laboratories, and new experiments that we report here.

3.1. Reactant Column Densities

Figure 1 of dB15 shows IR spectra of the authors' ice sample at 15 K before and after irradiation. Three reactants, N₂, H₂O, and CO₂, were identified and quantified by integrating selected IR features and then using IR band strengths (denoted A) to calculate column densities. More specifically, after integrating an absorbance band for the molecule of interest and converting to an optical depth scale by multiplying the result by $\ln(10) = 2.303$, one then divides the result by A for the IR band to get a molecular column density from the following equation:

$$N = \frac{2.303 \int_{\text{band}} (\text{Absorbance}) d\tilde{\nu}}{A}$$

This is a standard method, but for accurate results it requires the availability of appropriate band strengths (A) for the molecular components. With this in mind, we consider each of the three reactants of dB15.

The spectrum of the authors' unirradiated N₂+H₂O sample resembles that published by Ehrenfreund et al. (1996), with the exception of a large peak in the ν_3 region of CO₂ ($\sim 2340 \text{ cm}^{-1}$). The unstated assumption in dB15 was that the band strength of the ν_3 feature of crystalline CO₂ (Yamada & Person 1964) was applicable to CO₂ trapped in an N₂+H₂O ice, the result being a calculated $N_{\text{CO}_2} = 4.5 \times 10^{14} \text{ molecules cm}^{-2}$ for the ice's initial CO₂ column density. A different way to calculate CO₂ column density is to use IR peak heights. Figure 2 of Yamada & Person (1964) shows the spectrum of a CO₂ ice with a thickness $h = 2.39 \times 10^{-5} \text{ cm}$ (0.239 μm) and a peak absorbance of ~ 1.35 near 2340 cm^{-1} , from which an absorption coefficient of $\alpha = (2.303 \times 1.35/h) = 1.30 \times 10^5 \text{ cm}^{-1}$ is found. Returning to Figure 1 of dB15, the CO₂ peak's height is about 0.32 on an absorbance scale, so that the ice's equivalent CO₂ thickness is $h = (2.303 \times 0.32/\alpha) = 5.7 \times 10^{-6} \text{ cm}$ ($\sim 0.057 \mu\text{m}$). Using a CO₂ mass density of $\rho = 1.3 \text{ g cm}^{-3}$ (Satorre et al. 2008), the equivalent initial column density of carbon dioxide in dB15 is estimated to be $N_{\text{CO}_2} = h\rho N_A/44 = 1.0 \times 10^{17} \text{ molecules cm}^{-2}$, where $N_A = 6.022 \times 10^{23} \text{ CO}_2 \text{ molecules mol}^{-1}$. This N_{CO_2} value based on a peak height is about 200 times larger than the $4.5 \times 10^{14} \text{ molecules cm}^{-2}$ that was based on band area. A similar calculation with the optical constants of Hudgins et al. (1993) leads to a discrepancy of a factor of about 400.

Turning to N₂, an estimate for the band strength $A(\text{N}_2, 2328 \text{ cm}^{-1})$ is made in dB15, and the complication of H₂O ice being present is recognized. However, for an N₂+H₂O+CO₂ ice, additional difficulties arise because the strength of the N₂ fundamental near 2328 cm^{-1} depends strongly on the presence of CO₂ (Fredin et al. 1974). This means that given the large uncertainty in the CO₂ abundance just described, the choice for $A(\text{N}_2, 2328 \text{ cm}^{-1})$ also is highly uncertain. For a CO₂ column

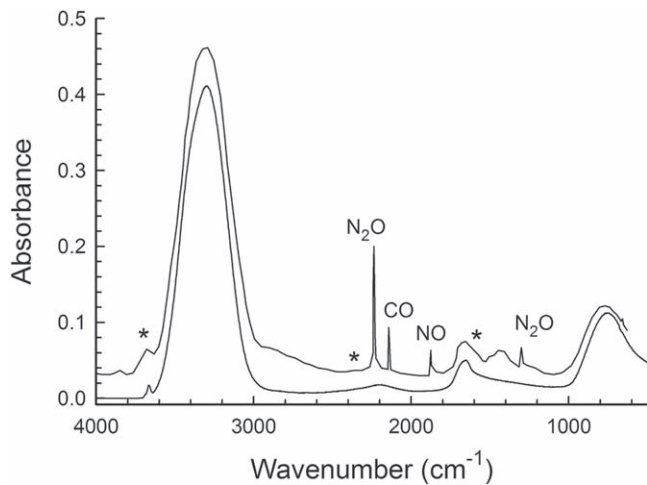


Figure 1. Lower spectrum was calculated (Swanepoel 1983) from the optical constants of Hudgins et al. (1993) for an amorphous H₂O ice at 10 K, with a thickness of 0.45 μm . The upper spectrum is from an ion-irradiated N₂+H₂O ice at 15 K, digitized from Figure 1 of de Barros et al. (2015) and offset for clarity. Asterisks indicate three regions, each about 50 cm^{-1} wide, of inaccurate digitization caused by overlapping lines in the original version. See the original publication for enlargements of several regions.

density that is uncertain by a factor of 200 (see above), Table 2 of Sandford et al. (2001) shows that $A(\text{N}_2, 2328 \text{ cm}^{-1})$ also can be off by about that much, drastically altering the calculated initial N₂ column density.

Admittedly these comments on the initial column densities for CO₂ and N₂ involve rough estimates, but the fact that they suggest values two orders of magnitude greater than those in dB15 is disconcerting. The differences might be from the choice of band strengths in dB15, the range over which IR bands were integrated (unstated), or the method of deconvolving bands that overlap (also unstated). The point is that such estimates, whether based on band areas or peak heights, require accurate band strengths or absorption coefficients, respectively, from appropriate standards. It is not clear that such laboratory data are available for N₂+H₂O or N₂+H₂O+CO₂ ices. Moreover, without accurate reactant abundances it is impossible to use the method of dB15 to extract quantitative kinetic information for radiation products.

The estimate for the initial H₂O column density in dB15 also is uncertain. The band strengths used can be traced to the work of Hagen et al. (1981) on amorphous H₂O, but it is not clear to what extent their values, and specifically the band strength of the 1655.2 cm^{-1} feature of H₂O ice, apply to H₂O trapped in N₂. There also is an inconsistency between the abundance ratio $(\text{N}_2/\text{H}_2\text{O}) = 10$, from the abstract and Figure 1 of dB15, and the $(\text{N}_2/\text{H}_2\text{O}) \approx 4.26$, calculated from data in the authors' Table 3.

The other spectrum in Figure 1 of dB15 is for the authors' N₂+H₂O ice after irradiation at 15 K. Our own Figure 1 compares that post-irradiation spectrum to one of amorphous H₂O ice at a similar temperature. Except for four sharp peaks and one broad feature near 1400 cm^{-1} in the upper trace, the two spectra are essentially identical. A strong, broad band at 3300 cm^{-1} is easily seen in both, as are weaker broad features at 1600 and 800 cm^{-1} . Taking the absorbance of the peak at 3300 cm^{-1} in the upper trace of our Figure 1 as 0.44, and assuming that it is from amorphous H₂O ice, the post-irradiation column density of H₂O can be estimated with the

method already applied to CO₂. The optical constant $k(\text{H}_2\text{O}, 3300 \text{ cm}^{-1})$ of Hudgins et al. (1993) gives $\alpha = 18,000 \text{ cm}^{-1}$, which yields $N_{\text{H}_2\text{O}} \approx 1.9 \times 10^{18} \text{ H}_2\text{O molecules cm}^{-2}$, about 380 times greater than the $N_{\text{H}_2\text{O}} = 5 \times 10^{15} \text{ H}_2\text{O molecules cm}^{-2}$ listed in Table 3 of dB15, and about 8 times larger than water's stated initial column density. One explanation for this discrepancy is that contamination from background or atmospheric CO₂ and H₂O in those experiments might have been greater than realized. This possibility could have been addressed by irradiating solid N₂ with no H₂O added (a control experiment) or through experiments using D₂O, but no such work was reported.

3.2. Identifications and Abundances of Reaction Products

Having illustrated some of the difficulties in determining abundances of reactants in low-temperature ices, we turn to reaction products observed in ion-irradiated N₂+H₂O ices by de Barros et al. (2015). Here too there are problems with abundances.

Thirteen reaction products are given in Table 2 of dB15, with 10 of them being quantified in later tables and figures. Two spectral peaks were shown for N₂O, and laboratory data were cited for their positions, so that the N₂O assignment seems secure. Only one NO peak was observed, corresponding to the molecule's fundamental vibration, and only one was reported for NO₂, but since both peaks are rather sharp, well defined, and well documented, their assignments can be taken as correct. Assignments of the remaining seven quantified products are more difficult. The azide radical (N₃) assignment might be correct, but see our Appendix C for questions about it. Ozone (O₃) is claimed as a product of irradiated N₂+H₂O, but only one IR peak was reported. Given the ease with which irradiated CO₂ produces ozone, that spectral assignment may be correct, but the O₃ might have come from CO₂ contamination and not from N₂+H₂O. Experiments using H₂¹⁸O could decide, but none were reported.

The remaining five quantified nitrogen–oxygen products are NO₃, N₂O₂, N₂O₃, N₂O₄, and N₂O₅. Their spectral assignments in dB15 tend to be based on single peaks that are weak, broad, and overlapping with other bands, and the citation often used for their IR positions and band strengths is a density-functional study of gas-phase nitrogen oxides (Stirling et al. 1994) that has not been checked for use with solid-phase data. Formation of other oxides is expected if NO, NO₂, and N₂O are present, but without additional support the authors' assignments to NO₃, N₂O₂, N₂O₃, N₂O₄, and N₂O₅ in dB15 are not secure and must be rejected.

The 10 quantified products in Table 2 of dB15 also are listed in our own Table 1, where it can be seen that there are significant problems that extend beyond peak positions. The problems include misidentifications (e.g., N₃ versus N₃⁺; Dyke et al. 1982), information missing from the papers cited (e.g., N₂O₂, N₂O₄), disagreement of spectral positions with the literature (e.g., NO₃, N₂O₅), mistakes in copying from the literature (e.g., NO₂, N₂O), and the use of gas-phase band strengths to interpret solid-phase results (many). Here we consider band strengths of just two compounds, the first and last ones listed in Table 1.

The IR band strength of N₃ used by dB15 is particularly important, as it influences the authors' claim that N₃ is the most abundant product in their experiments. However, the band strength selected is from a reflection-transmission method and

Table 1
Comments on Table 2 of the N_2+H_2O Study of de Barros et al. (2015)^a

Molecule	Comments on Assignments and Band Strengths
N_3	The first peak listed is incorrectly assigned. It is not from the N_3 radical, but from the N_3^+ cation. The other band strengths (A) listed are based on an estimate from a reflection-transmission type IR spectrum, and the accuracy of that estimate has not been checked.
NO	The position and A given for the first peak are not in the paper cited, and in any case that paper reports a gas-phase calculation, not a solid-phase measurement. The source listed for the second $A'(NO)$ has no details about the measurement and only an incomplete reference in a table.
NO_2	The band strength selected for use is not in the <i>Icarus</i> paper cited. (Also, the wrong volume and year are given for that reference.) The other band strength given was miscopied and is 10 times too large.
NO_3	The spectral position disagrees with the literature (Beckers et al. 2009) by about 25 cm^{-1} , making this one-peak spectral assignment questionable. The A value listed is from a gas-phase calculation.
N_2O	The band strength selected for use is from a gas-phase calculation, not a solid-phase measurement. The other three A values listed are from a mixed amorphous-crystalline ice. The $A(2573.3\text{ cm}^{-1})$ value was miscopied and is 10 times larger than in the original publication.
N_2O_2	The band strength selected for use is from a gas-phase calculation, not a solid-phase measurement. The first peak's position is not in the paper cited. The second peak listed is not in the work cited, which is not about N_2O_2 .
N_2O_3	The N_2O_3 assignment is based on just one peak, which is either incorrectly labeled in Figure 2(d) or incorrectly assigned. The band strength listed is from a gas-phase calculation.
N_2O_4	One band strength is not in the paper cited, which is not about N_2O_4 . The other band strength is from a gas-phase calculation, not a solid-phase measurement.
N_2O_5	The N_2O_5 assignment is based on a single peak about 30 cm^{-1} lower than in the reference cited. Again, the A value is from a gas-phase calculation, not a solid-phase measurement.
O_3	Measurement of the band strength listed is not in either of the papers cited.

Note.

^a In earlier work we have drawn a distinction between absolute (A) and apparent (A') IR band strengths (e.g., Hudson et al. 2014). For simplicity, in this paper only A is used.

is not readily transferable to a conventional transmission measurement (Hudson & Moore 2002). The result was $A(N_3, 1657\text{ cm}^{-1}) = 7.2 \times 10^{-20}\text{ cm molecule}^{-1}$, which contrasts sharply with a later value of $4.0 \times 10^{-17}\text{ cm molecule}^{-1}$, calculated with density-functional methods (Jamieson & Kaiser 2007). Depending on which value is selected, N_3 can be interpreted as either one of the more abundant or one of the least abundant products in irradiated N_2+H_2O ices.

The quantification of ozone (O_3) is another problem. The ozone band strength in Table 2 of dB15 is $A(O_3, 1039.7\text{ cm}^{-1}) = 1.40 \times 10^{-17}\text{ cm molecule}^{-1}$, but details cannot be found in the two papers cited. Loeffler et al. (2006) reported only an effective A value for the experiments they carried out with a reflection-transmission arrangement. The Sicilia et al. (2012) paper cited by dB15 gives only “Smith et al. (1985)” in a table as the source of the O_3 band strength, with no citation in the list of references. Our own literature search eventually determined that Smith et al. (1985) is a book chapter that cites even earlier work for $A(O_3, 1039.7\text{ cm}^{-1})$. Additional searching finally revealed the original reference to be Secroun et al. (1981), who published the result of a gas-phase measurement for O_3 at 300 K. Our calculation from the latter paper gives $A(O_3, 1039.7\text{ cm}^{-1}) = 1.48 \times 10^{-17}\text{ cm molecule}^{-1}$, slightly higher than the value in dB15.

To summarize, of the 10 reaction products quantified in Table 2 of dB15, the NO, NO_2 , and N_2O assignments seem secure. The N_3 and O_3 assignments also are probably correct, although a few questions remain. The remaining five assignments are questionable due to a lack of supporting data. Of the 10 band strengths used for radiation products, eight are suspect, as they are from calculations on gas-phase molecules and have not been checked for use with ices, one seems to be miscopied, and one is from a different type of measurement. We conclude that the band strengths used in dB15 for reaction products are on such uncertain ground that their application to kinetic data and reaction yields in ices is highly questionable, significantly

lowering the accuracy and value of that paper's extensive numerical results (i.e., cross sections, abundances, and reaction yields). Also, without accurate abundances one cannot expect calculations of elemental budgets to yield meaningful results.

3.3. Proposed Tracers for Astronomical CO_2 and N_2+H_2O

Among the conclusions drawn by dB15 (page 12) is the following: “Comparing the current results with those of Boduch et al. (2012), it seems that ozone is a good indicator for the presence of molecular oxygen, while nitrogen oxides give the best indication of the presence of molecular nitrogen mixed with water.” Ozone certainly is made from molecular oxygen, but other sources exist, including CO_2 . As for nitrogen oxides, our Figure 2 shows IR spectra we recorded before and after the 1 MeV H^+ irradiation of N_2+O_2 (100:1) at 12 K. The spectrum of the irradiated ice (upper trace) shows sharp peaks from the formation of N_2O (2235 cm^{-1}), NO (1874 cm^{-1}), NO_2 (1615 cm^{-1}), and O_3 (1042 cm^{-1}). Less obvious are smaller peaks for N_3 (1657 cm^{-1}) and O_3 (2116 and 704 cm^{-1}). In Table 2 we list IR assignments for N_3 , NO, NO_2 , N_2O , and N_2O_2 , supported by $^{15}N_2$ experiments and reference spectra recorded in our laboratory. Literature results are included for comparison. Our O_3 assignment in Figure 2 was confirmed in a similar way, multiple O_3 peaks being observed and with positions that agreed with reference spectra we recorded. From all of these observations we conclude that nitrogen oxides observed in an irradiated N_2 -rich ice cannot be used to infer a previous composition of N_2+H_2O in either a laboratory or an astronomical environment.

Identifications of the higher nitrogen oxides, N_2O_3 , N_2O_4 , and N_2O_5 , in our experiments and those of others are more problematic, as each compound absorbs in the $1860\text{--}1620\text{ cm}^{-1}$, $1320\text{--}1220\text{ cm}^{-1}$, and $850\text{--}650\text{ cm}^{-1}$ regions marked by the asterisks in Figure 2. Our Figure 3 shows an example of the spectral confusion one meets. Going

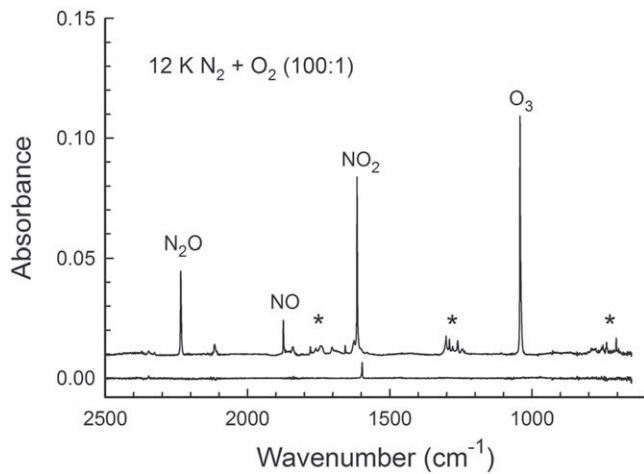


Figure 2. IR spectra of an N_2+O_2 (100:1) ice at 12 K before (lower) and after (upper) irradiation by 1 MeV H^+ to a fluence of about $1 \times 10^{14} H^+ cm^{-2}$. A small peak near $1600 cm^{-1}$ in the lower spectrum is from trapped H_2O ($N_2:H_2O \sim 2400:1$). Asterisks mark three regions of overlapping IR bands of nitrogen oxides. See the text. The sample's original thickness was about $3 \mu m$. The upper spectrum has been offset for clarity.

Table 2

Infrared Identifications of Products with Two to Four Atoms from 1 MeV H^+ Irradiation of N_2+O_2 (100:1) Ice at 12 K

Molecule	Mode	Position (cm^{-1})		^{15}N Shift (cm^{-1})	
		This Work	Literature	This Work	Literature
N_3	ν_1	1657	1657 ^a	54	54 ^a
NO	ν_1	1874	1875 ^b	33	33 ^b
NO_2	$\nu_1 + \nu_3$	2908	2905 ^c	46	47 ^d
	ν_3	1615	1616 ^c	35	37 ^d
N_2O	ν_2	750	750 ^e	10	9.6 ^d
	ν_3	2235	2236 ^f	70	70 ^f
$cis-N_2O_2$	ν_1	1291	1291 ^f	20	20 ^f
	ν_1	1866	1866 ^b	...	32.9 ^b
$trans-N_2O_2$	ν_5	1779	1780 ^b	31	31.5 ^b
	ν_5	1760?	1760 ^b	...	31.1 ^b

Notes.

^a Tian et al. (1988); N_2 matrix.

^b Krim (1998); N_2 matrix.

^c Varette & Pimentel (1971); N_2 matrix.

^d Arakawa & Nielsen (1958); gas phase.

^e St. Louis & Crawford (1965); O_2 matrix; overlaps slightly with a feature of N_2O_4 .

^f Łapinski et al. (2001); N_2 matrix.

^g Overlaps with other features or too weak for accurate measurement.

from spectrum (a) before irradiation to (b) after the first dose, three sharp peaks of comparable height are seen. These are assigned to N_2O_3 , N_2O , and N_2O_4 , with a smaller feature for N_2O_5 , based mainly on ^{15}N isotopic shifts observed in an $^{15}N_2+O_2$ experiment and comparisons with the literature. Results for these three oxides are summarized in Table 3, but without appropriate reference spectra, the assignments are slightly more tentative than those in our Table 2. Also, the overlap of the many IR bands of these molecules makes some of their ^{15}N shifts difficult to measure. Four peaks are marked with numbers in Figure 3, but their assignments would be even less certain, such as the possibility that (iii) is from iso- N_2O_4 and (iv) is from NO_2^- . Our goal was not to assign every IR peak, but rather to obtain evidence that N_2O_3 , N_2O_4 , and N_2O_5

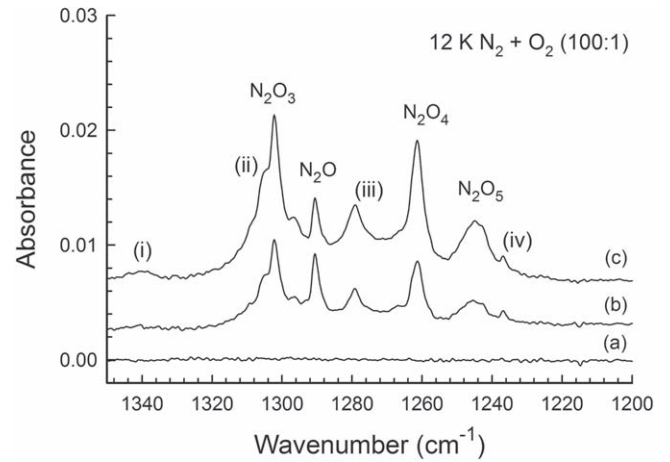


Figure 3. IR spectra of an N_2+O_2 (100:1) ice at 12 K (a) before and after irradiations by 1 MeV H^+ to a fluence of about (b) 1×10^{14} and (c) $2 \times 10^{14} H^+ cm^{-2}$. See the text for comments on (i)–(iv). The sample's original thickness was about $3 \mu m$. The spectra have been offset for clarity.

Table 3

Infrared Identifications of Products with Five to Seven Atoms from 1 MeV H^+ Irradiation of N_2+O_2 (100:1) Ice at 12 K

Assignments Slightly More Tentative than Those in Table 2					
Molecule	Mode	Position (cm^{-1})		^{15}N Shift (cm^{-1})	
		This Work	Literature	This Work	Literature
asymm N_2O_3	ν_1	1841	1840 ^a	32	32 ^a
	ν_2	1630	1630 ^a	32?	36 ^a
	ν_3	1302	1302 ^a	15	16 ^a
N_2O_4	ν_{11}	1261	1261 ^a	12	11 ^b
	ν_{12}	751 (weak)	751 ^a	~11	11 ^b
N_2O_5	ν_1	~1740	1742 ^c	~35	40 ^c
	ν_9	1703	1702 ^c	39	40 ^c
	ν_{10}	1245	1245 ^c	6	8 ^c
	ν_{11}	738	732 ^c	9	8.5 ^c

Notes.

^a Varette & Pimentel (1971) N_2 matrix.

^b Begun & Fletcher (1960) gas phase.

^c N_2O_5 literature values are from Bencivenni et al. (1996) with some reassignments by Zhun et al. (1996) Ar matrix.

are radiation products. Future work will address assignments to specific isomers, such as *cis*- and *trans*- N_2O_2 , asymmetric and symmetric N_2O_3 , N_2O_4 , and iso- N_2O_4 , and ions such as NO^+ , NO_2^+ , NO_2^- , and NO_3^- (e.g., Terenishi & Decius 1954; Forney et al. 1993). However, it is clear that prolonged irradiation of N_2 -rich ices can produce a wide range of nitrogen oxides.

3.4. Isotopic Enrichment of ^{15}N and the IR Spectrum of N_2

Two other results reported by de Barros et al. (2015) concern the mid-IR spectrum of N_2 and a striking ^{15}N isotopic enrichment produced by ion irradiation of an N_2 -rich ice. See our Appendices B and C for a detailed analyses of these results.

4. Discussion

From the preceding section we conclude that many of the IR band strengths used to quantify product yields in such solids are of questionable relevance, having never been checked against

Table 4
Nitrogen Oxidation Numbers for Selected Molecules and Ions^a

Nitrogen Oxidation Number	Molecules and Ions			
0	N ₂			
+1	N ₂ O			
+2	NO	N ₂ O ₂		
+3	N ₂ O ₃	NO ⁺	NO ₂ ⁻	HNO ₂
+4	NO ₂	N ₂ O ₄		
+5	N ₂ O ₅	NO ₂ ⁺	NO ₃ ⁻	HNO ₃
+6	NO ₃			

Note.

^a The nitrogen atom in N, NH, NH₂, and NH₃ has an oxidation number of 0, -1, -2, and -3, respectively.

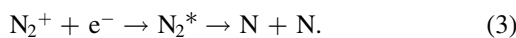
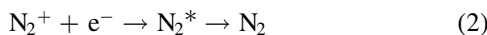
solid-phase samples. However, our laboratory work strongly supports the claims of de Barros et al. (2015) and others of N₃, NO, NO₂, and N₂O formation by radiation processes. Here we first address reaction chemistry in N₂-rich ices and follow with some comments on reaction products, radiation doses, chemical kinetics, and astronomical connections.

4.1. Reaction Chemistry in N₂-rich Ices

Suffice it to say that the chemistry of irradiated N₂-rich mixtures is complex and its study has a long history. Perhaps the earliest relevant observation is that of Soddy (1911), who noted the formation of N₂O in irradiated air. However, the chemical evolution of irradiated N₂+O₂ gas mixtures seems to have first been investigated by Lind & Bardwell (1929), who found that if sufficient O₂ is present, then nitrogen oxidation will transform N₂ into NO and then into NO₂. If H₂O is present, then it will convert NO₂ into nitric acid, HNO₃. Table 4 shows the rise in nitrogen oxidation number for this N₂ → NO → NO₂ → HNO₃ sequence. In the late 1950s, Jones (1959) identified and quantified both NO₂ and N₂O as radiation products of N₂+O₂+H₂O mixtures, and Hardeck & Dondes (1958) reported the radiolytic formation of N₂O₅. By the 1970s, Willis and coworkers were able to list dozens of reactions in their papers on the irradiation of nitrogen–oxygen mixtures, many such studies being motivated by applications to nuclear facilities (Willis et al. 1970; Willis & Boyd 1976).

Despite all of this earlier work, it is not obvious a priori which of the many reactions occurring in irradiated N₂-rich gases are most relevant to the ices we have studied, but some processes seem beyond question. It also seems clear that both ionic and free-radical reactions are important and that the restricting environment of the solid state (i.e., the cage effect) will encourage more recombinations than in the gas phase.

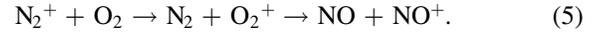
A hallmark of radiation chemistry is that the action of the ionizing agent is nonspecific, and so incident radiation acting on an N₂+O₂ mixture will influence both components. In our irradiated ices, since N₂ is the more abundant component, the nitrogen molecular ion N₂⁺ is expected to be one of the primary radiation products. Its neutralization can regenerate N₂ and, if that event is sufficiently energetic, yield N atoms. See reactions (1)–(3) below:



Accompanying reactions (2) and (3) will be the reaction of N₂⁺ with the O₂ present, giving nitric oxide (NO):



Since the ionization energy of N₂ is slightly higher than that of O₂, a more accurate sequence might be



Reaction of the N₂⁺ made in reaction (1) with the N₂ matrix will produce the nitrogen dimer radical cation, N₄⁺ (Varney 1953). Many reactions other than neutralization can follow, one being the combination of N₄⁺ with an O₂ anion (O₂⁻) to give both N₃ and NO₂ as follows:



The neutral molecular products of reactions (4)–(8), other than N₂, are N₃, NO, and NO₂ and are easily seen in our spectra. Note that the positions of the strongest ¹⁴N₄⁺ and ¹⁵N₄⁺ IR features are near the most intense IR peaks for ¹⁴N₂O and ¹⁵N₂O, respectively, making the direct IR detection of N₄⁺ challenging (Thompson & Jacox 1990; Savchenko et al. 2014).

The preceding is based on reactions involving ions, but neutral free radicals also are important. As already stated, during an irradiation with MeV ions a track of excitations and ionizations will be produced by each ion as it travels through an ice, generating secondary electrons that produce their own trails of chemical change. The excitation and dissociation of N₂ represented as



can be followed by



again to make the N₃ we observed, although more complex paths to N₃ exist (Mencos et al. 2017). For N₂-rich ices containing O₂, excitation and dissociation of molecular oxygen will give O atoms from which nitrous oxide and ozone can form in reactions (11)–(13):



by O-atom addition (DeMore & Davidson 1959). If H₂O is present, then it too will be a source of O atoms, from which reaction (12) will follow (Zheng et al. 2011). Radiolysis of the N₂O produced will give the reverse of reaction (12), but it will also yield nitric oxide (NO) as shown below:

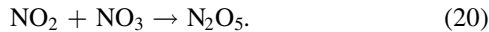
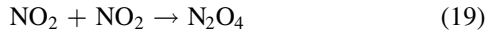
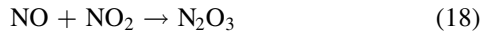


Several neutral oxidants exist in irradiated N₂+O₂ ices, specifically O, O₂, and O₃, and these can lead to more complex oxides. For example, starting from NO gives



although we have no firm evidence for NO₃. Additional radical–radical reactions will lead to the more complex oxides

seen in our IR spectra:



See Minissale et al. (2014) and Ioppolo et al. (2014) for similar reactions in a different context. See Cocke et al. (2004) and references therein for solid-phase N_2O_5 formation without NO_3 . Note that such radical–radical combinations are expected to proceed with no electronic activation barrier, being restricted mainly by their positions and mobility within the irradiated ice. Other possible reactions include, if sufficient energy is available, O-atom transfer from O_2 and especially O_3 . See Koch et al. (1995) for a different path to N_2O_5 , from which nitric acid (HNO_3) can be made by reaction with H_2O .

The formation of N_2O has been described, so it is appropriate to mention that that molecule’s radiation chemistry also has been studied for nearly a century (Wourtsel 1919). Sambrook & Freeman (1974) reported that the major radiolytic products from N_2O include N_2 , O_2 , NO , and NO_2 , the last three being secondary products in an ice initially composed of $\text{N}_2+\text{H}_2\text{O}$. Oxygen atoms from N_2O radiolysis will react to form NO according to



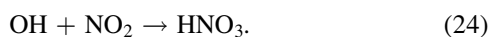
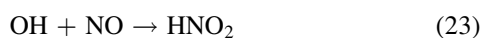
and from NO the other oxides already mentioned, as well as O_3 , will follow, as already described. Similar arguments can be made for the formation of N_2O , NO , NO_2 , and O_3 , from other starting ice mixtures, such as N_2+CO_2 .

The complication added by the presence of CO_2 in the irradiated ices of dB15 is that it is a second source of O , O_2 , and O_3 , which will participate in many of the reactions already written. Also produced will be CO , which we suspect is the source of the peak near 2140 cm^{-1} in Figure 1 of dB15, but unlabeled, and also seen in the upper spectrum of our own Figure 1. However, the participation of CO_2 jeopardizes any interpretation of the resulting kinetic information and product yields solely in terms of $\text{N}_2+\text{H}_2\text{O}$ chemistry.

Note that all of the reactions in this section have ignored complications from electronic spin states, about which our methods provide no information. See the papers of Willis and coworkers for more complex versions of most of these reactions with spin explicitly included (Willis et al. 1970; Willis & Boyd 1976).

4.2. Other Possible Reaction Products from $\text{N}_2+\text{H}_2\text{O}$

Since N atoms are made by the irradiation of $\text{N}_2+\text{H}_2\text{O}$, and since both H and OH can form from H_2O , there are multiple possibilities for radical–radical reactions, such as



The above three products are mentioned in dB15, but without reference spectra it is difficult to make firm assignments. Similarly, N and H atoms might react to make NH , NH_2 , and NH_3 , or the NH radicals might be captured by the N_2 matrix to make HN_3 . On page 9 of dB15 it is said that HN_3 “bands were

investigated,” but no details were provided. It is not known whether the authors looked up gas-phase positions of HN_3 IR features, whether they prepared solid mixtures of HN_3 in N_2 and recorded their IR spectra, or whether something else was done. Van Thiel & Pimentel (1960) showed that the strongest IR feature of solid HN_3 is in the same region where CO absorbs, and so it could overlap, mask, or be masked by CO ’s fundamental band. Without appropriate reference spectra, little more can be said except that the CO label in our Figure 1 could be a simplification.

4.3. Reaction Products and Radiation Types

Table 5’s first four lines list some results from radiation experiments with N_2 -rich ices in four different laboratories. A recent study of a more complex ice also is included (Vasconcelos et al. 2017). All five studies are seen to have reported radiolytic formation of NO , NO_2 , and N_2O , suggesting that if N_2 and a source of oxygen are present, then the ice can be driven to the same nitrogen oxides. One can safely predict that the same products will be observed from other irradiated nitrogen-rich ices, such as N_2+O_3 , NH_3+O_2 , and so forth. For completeness, an ion-implantation study of Boduch et al. (2012) should be mentioned here. It included two IR spectra of N_2+O_2 after irradiation by $30\text{ keV }^{13}\text{C}^{2+}$ at 15 K, but neither an initial N_2 -to- O_2 ratio nor a radiation dose was given, and so that work is not included in our Table 5, although it too reported NO , NO_2 , and N_2O formation.

The third column of Table 5 shows that radiations with a wide range of stopping powers were used in the five experiments listed. Since the composition of the ice of de Barros et al. (2015) was uncertain (*vide supra*), the stopping power of 40 MeV Ni^{11+} in solid N_2 was calculated ($3600\text{ keV } \mu\text{m}^{-1}$) and is listed in Table 5. It is readily seen that in that experiment the energy deposition per unit distance was about 300% greater than the next largest value, raising the chances of sample heating and of sputtering, both of which would cause N_2 loss. This might explain why the post-irradiation spectrum of $\text{N}_2+\text{H}_2\text{O}$ in our Figure 1 so closely resembles that of unirradiated amorphous H_2O ice. With such a substantial N_2 loss in the 40 MeV Ni^{11+} experiment, it is difficult to unravel the underlying reaction chemistry because the ice changes from being dominated by nonpolar N_2 molecules to being composed of the highly polar H_2O and reaction products. The chemical reactions occurring at the experiment’s start play an increasingly smaller role as the radiolysis proceeds, and little or no role near its end.

4.4. Reaction Kinetics in $\text{N}_2+\text{H}_2\text{O}$ Ices

A problem with trying to understand chemistry in ices, in either a laboratory or astronomical setting, is that it can be hard to isolate specific reactions for study, so that a phenomenological approach is often necessary. For the $\text{N}_2+\text{H}_2\text{O}$ ice of interest here, no reactions were written by dB15 for this mixture’s chemical evolution. The authors presented a set of equations similar to those for a reversible reaction that follows first-order kinetics in both directions. A solution for this system has long been known (Harcourt & Esson 1866) and suggests that a semi-log plot of $N_t - N_\infty$ over time (N = reactant abundance) should be linear with a slope that is the sum of the forward and reverse rate constants. An assumption of parallel nonreversible destruction reactions would give a different

Table 5
Examples of Reports of Radiation Products in Cosmic Ice Analogs^a

Publication	Experimental Conditions	Stopping Power (keV μm^{-1})	NO	NO ₂	N ₂ O
Jamieson et al. (2005)	5 keV e ⁻ N ₂ +CO ₂ (1:1), 10 K	6.4 ^b	✓	✓	✓
Sicilia et al. (2012)	200 keV H ⁺ N ₂ +CO (8:1), 16 K	57 ^c	✓	✓	✓
de Barros et al. (2015)	40 MeV Ni ¹¹⁺ N ₂ +H ₂ O (10:1), 15 K	3600 ^d	✓	✓	✓
This work	1 MeV H ⁺ N ₂ +O ₂ (100:1), 12 K	20 ^d	✓	✓	✓
Vasconcelos et al. (2017)	15.7 MeV O ⁵⁺ N ₂ +H ₂ O+CO ₂ +NH ₃ (100:1.5:0.2:0.4), 16 K	944 ^c	✓	✓	✓

Notes.

^a The ✓ symbol indicates that the product was reported by the authors.

^b Linear energy transfer reported by the authors.

^c Value reported by the authors.

^d Calculated for pure N₂ for the ion and energy listed.

solution, and consecutive reactions would give yet a different result. Regardless, an explicit description of the kinetic system assumed to be relevant, to include specific reactions and the order of each, is critical for extracting accurate rate information from the laboratory data. Mathematical equations with adjustable parameters certainly can be used to fit data points, but without a basis in the chemistry of the system, the parameters extracted are not necessarily rate constants that are applicable to other chemical systems. See Rodiguin & Rodiguina (1964), Capellos & Bielski (1972), and Andraos (1999) for examples of complex kinetic systems and solutions by Laplace and Laplace–Carson transforms.

Given the preceding observations and results, we conclude that although a full kinetic analysis to extract rate constants for the N₂+H₂O system is of interest, it is impossible at present given the uncertainty over possible ice contaminants (i.e., CO₂, H₂O), convincing assignments of some of the IR features of products, and the lack of accurate product column densities.

4.5. Some Astrochemical Considerations

Having examined some results from N₂-rich ices in our lab and elsewhere, we consider some astrochemical implications. First and foremost is the ease of formation of nitrogen oxides in a variety of chemical systems. The N₂+CO₂, N₂+CO, N₂+H₂O, and N₂+O₂ combinations have been studied in four independent laboratories and found, from the action of ionizing radiation, to produce N₂O, NO, and NO₂, and probably more complex nitrogen oxides. Again, see Table 5, which also includes the four-component ice recently studied by Vasconcelos et al. (2017). These same products can be expected in irradiated ices of TNOs that are N₂ rich. Although these three oxides might be observed spectroscopically in the gas phase, direct detection in ices could be difficult. In any case, radiolytic oxidation in solid N₂ would seem to be firmly established.

A related implication of the ease of forming nitrogen oxides is that small amounts of H₂O in N₂-rich ices will be consumed by radiation-driven chemistry. This makes it challenging to identify H₂O mixed with N₂-rich ices on TNOs, such as Pluto. The clearest detections to date are the broad and weak, but distinct, near-IR features of H₂O ice observed with the *New Horizons* fly-by mission (Grundy et al. 2016).

In contrast to the situation for N₂-rich TNOs, that for trans-Neptunian objects that are rich in solid NH₃, such as Charon, is less clear. Free-radical reactions can dominate in nonpolar ices, such as those studied here, but icy solids rich in polar molecules, like NH₃, likely would find a larger contribution from ions, such as NH₄⁺, and electron-transfer reactions. The

Table 6
Radiation Doses for Ices of Three Astronomical Objects^a

Object	Time	Distance	Depth	Dose (eV/ 16 amu)	Dose (eV/ 28 amu)
Pluto	4.6 Gyr	~40 au	1 m	30	52.5
TNO	4.6 Gyr	~1000 au	1 m	50	87.5
Dense IS Cloud	10 ⁶ yr	...	0.02 μm	0.3	0.525
Dense IS Cloud	10 ⁷ yr	...	0.02 μm	3	5.25

Note.

^a Based on Moore et al. (2001), Moore & Hudson (2005), Hudson et al. (2008), and references therein. The 0.02 μm depth for an interstellar ice grain considers both the entrance and exit layers. See Moore et al. (2001).

reason for this is that an ionization, such as N₂ → N₂⁺ + e⁻, involved in a radiolytic reaction scheme is more likely to be followed by electron-cation recombination in nonpolar solids than in those of higher dielectric constant where the cation and e⁻ are, in a sense, shielded from one another (Williams 1964; Swallow 1973, p. 77; Mozumder 1999, pp. 232–234). Seen this way, one can predict quite different chemistries for Pluto and Charon owing to their different surface ices.

In previous papers, we estimated proton radiation doses for multiple astronomical objects and environments (Moore et al. 2001; Moore & Hudson 2005; Hudson et al. 2008, and references therein). Table 6 summarizes some of our estimates, with doses being given for both 16 and 28 amu scales, the latter being the more relevant for the N₂-rich ices of the present work. The table’s final column shows that the dose of ~1 eV (N₂ molecule)⁻¹ for our Figure 2 is reasonable for a 1 m depth on Pluto over ~90 Myr and for a 1 m depth over ~50 Myr for more distant TNOs. Each orbit of Pluto is accompanied by the sublimation of N₂-rich surface material, which can carry nitrogen-oxide radiation products into the gas phase, but also can lead to the enrichment of the less volatile nitrogen oxides left behind on the surface. This suggests that the greatest abundance of gas-phase nitrogen oxides from Pluto might well be found near perihelion.

For interstellar ices, Table 6 shows that the ice mantles on interstellar grains receive a dose of a few eV per N₂ molecule over the lifetime of a dark cloud (10⁶–10⁷ yr), an estimate that compares well to that of Sicilia et al. (2012). This dose is similar to that used in experiments that we and others have carried out. Since our estimates consider only H⁺, the most abundant component of cosmic rays, the actual dose might be

somewhat higher. This strengthens the possibility (Zheng et al. 2008) that N_2 mixed with H_2O -rich ices in interstellar grain mantles can be radiolytically oxidized and so might never be observed in the solid state as N_2 . In such cases, any nitrogen present might exist as NO , NO_2 , N_2O , or maybe NO_2^- and other ions. See Halfen et al. (2001) for a study of gas-phase NO and N_2O in the Sagittarius B2 interstellar cloud.

A slightly different picture emerges for apolar interstellar ices, which are thought to have a relatively high abundance of N_2 and O_2 (Ehrenfreund et al. 1998). Radiation-driven reactions would yield products from our Tables 2 and 4, with any H_2O trapped in such ices, at low abundance, also succumbing to radiation-driven chemistry. In apolar ices, O atoms would react with N_2 to make N_2O and other products, perhaps helping to explain why O_3 has not yet been identified as an interstellar molecule.

5. Summary and Conclusions

1. The IR band strengths used in de Barros et al. (2015) to quantify the radiation products of an N_2+H_2O ice vary from unchecked to suspect, casting doubt on the authors' subsequent data analyses.
2. Nitrogen oxides cannot be used as tracers of N_2+H_2O ices.
3. Conversely, by combining new work from our laboratory (see, e.g., Table 5) with results from elsewhere, we have shown that the irradiation of N_2 -rich icy solids readily produces the simpler nitrogen oxides, N_2O , NO , and NO_2 .
4. An extensive array of spectroscopic tools and techniques are available and required for firm assignments in the IR spectra of interstellar and planetary ice analogs, particularly if those spectra contain broad, overlapping bands. Such aids include isotopic substitution, thermal annealings, control experiments (blanks), comparisons with similar chemical systems, careful attention to the underlying chemistry, and reference spectra recorded under the same conditions, and preferably with the same equipment, used for the ices being studied.
5. Detailed kinetic results should be accompanied by a statement of the reaction order(s) and types of reactions assumed since kinetic order determines the mathematical relations used for curve fits and the extraction of rate constants.
6. IR studies of solid nitrogen oxides, in the laboratory and elsewhere, are hindered by the lack of appropriate reference spectra. New measurements of IR band strengths and optical constants for nitrogen oxides also are needed before studies of the low-temperature formation of these compounds in amorphous ices can be quantified. Claims of nitrogen-oxide formation and quantification in ices should be judged with this in mind. Unfortunately, since many nitrogen oxides are both toxic and detrimental to laboratory equipment, continued slow progress is expected.

In our appendices we justify the following concluding statements:

1. The report (de Barros et al. 2015) of an IR band near 2347.5 cm^{-1} for solid N_2 conflicts with the bulk of the spectroscopic literature and is unsupported by the results presented to date. Astronomical searches for solid N_2

should continue to focus on the molecule's well-known fundamental and first-overtone bands.

2. The striking and specific ^{15}N enrichment reported for N_3 seems highly unlikely and conflicts with published results on N_3 formation in radiation experiments.

This work was supported by NASA's Planetary Science Division Internal Scientist Funding Program through the Fundamental Laboratory Research (FLaRe) work package at the NASA Goddard Space Flight Center. Also acknowledged is the NASA Astrobiology Institute through funding to the Goddard Center for Astrobiology under proposal 13-13NAI7-0032. Stephen Brown, Eugene Gerashchenko, and Martin Carts of NASA Goddard's Radiation Effects Facility are thanked for the operation and maintenance of the Van de Graaff accelerator. Many helpful conversations with Marla Moore and Perry Gerakines are acknowledged.

Appendix A

During the course of this study, a relatively large number of questionable items were found in a paper published in this journal by de Barros et al. (2015). For example, on page 2 in the second column, the units of stopping power are incorrect, or at least ambiguous. The IR spectra of Figure 1 on page 2 for two N_2+H_2O mixtures are not compared to spectra published earlier by Ehrenfreund et al. (1996). On page 3, the order of the line types in the legend at the top of Figure 2 disagrees with the top three panels in the figure itself. Figure 2(d) has a peak near 1875 cm^{-1} labeled N_2O_3 , but Table 2 gives 1834.2 cm^{-1} as the position. On page 3 in the second column, a spectral band is designated $\nu_1 + \sigma$, but that label's meaning is never explained. The last sentence on page 3 employs "blueshift" in a sense that is opposite to conventional usage, and "wavelength" is used where "wavenumber" is meant. On page 4, the first entry in Table 1 is attributed to the lead author's previous work and one other paper, but the measurement cited is originally from Hagen et al. (1981). Five rows later, the " ν_2 monomer" assignment should be designated " ν_1 monomer" instead, unless the band position (3633.3 cm^{-1}) is in error. Further, the 3723.8 and 3633.3 cm^{-1} peaks in that table are from isolated H_2O (Van Thiel et al. 1957), not from dangling OH bonds (Rowland et al. 1991). On page 4 in the first column, 9.8×10^{17} is considered to be "almost one order of magnitude higher" than 2.3×10^{17} . On page 6 in the first column, the last paragraph's ^{18}CO should be $^{18}CO_2$ instead. Also on page 6 in the first column, the ratios 2200 and 220 are really 2200 and 511 according to Table 3. At the top of page 9, the *cis* and *trans* isomers of N_2O_2 are noted and data for them are plotted in Figure 6, but the wavenumbers of the peaks used to follow those two molecules and generate the points plotted are not unequivocally stated. Figure 6's caption refers to some of the curves in the figure as predictions. They are, in fact, curve fits used to extract kinetic information from the lab measurements, as opposed to being a priori mathematical statements.

Appendix B

B.1. Infrared Features of Molecular Nitrogen (N_2)

The N_2 abundance in planetary and interstellar ices is of considerable interest and importance, and so the IR absorbance

of solid N₂ has been studied for applications to both the ISM (Sandford et al. 2001) and the outer solar system (Tryka et al. 1995). However, isolated N₂ molecules are IR-inactive, and solid N₂ has only weak IR activity, hindering its astronomical detection by IR methods. This means that the discovery of a new N₂ IR feature would be of great interest.

Figure 1 and Table 1 of dB15 have an IR peak near 2347 cm⁻¹ that is labeled N₂+CO₂, with a component at 2347.5 cm⁻¹ that the authors assigned to N₂. However, no such position is known for N₂, and the authors' assignment is not supported with either their own reference spectra or isotopic substitution experiments (e.g., ¹⁵N₂). Further, no IR spectra are shown of either the unirradiated ice at multiple temperatures or ices with different N₂:H₂O ratios, which might clarify the proposed N₂ assignment. The author's Table 1 cites a 1999 paper of Hadjiivanov & Knözinger (1999) for an N₂ peak in that region, but that paper's experimental conditions (adsorption on a zeolite at 7.5 torr) differ significantly from those in dB15 (bulk N₂ ice under vacuum). A paper of Zheng et al. (2008) also is cited for support, but those authors give only a footnote in a table of their own that cites an unpublished calculation for an IR peak at 2374 cm⁻¹ to assign a feature at 2348 cm⁻¹ in irradiated NH₃, again with no reference spectra provided. Finally, the band strength $A = 1.5 \times 10^{-20}$ cm molecule⁻¹ calculated in dB15 for the IR feature at 2347.5 cm⁻¹, which the authors assigned to solid N₂, is about seven times (~600%) larger than the band strength of the N₂ fundamental near 2328 cm⁻¹. Therefore, since an overtone was seen for the 2328 cm⁻¹ peak, one is expected for the much stronger 2347.5 cm⁻¹ feature, but none was reported. Reference spectra of N₂-rich ices (e.g., Fredin et al. 1974; Bernstein & Sandford 1999), as well as spectra showing N₂ formation in irradiated NH₃ (Bordalo et al. 2013), all give the position of the N₂ fundamental vibration as near 2328 cm⁻¹, not 2347.5 cm⁻¹, and so it is not clear to what N₂ vibration the latter could apply.

The more likely explanation for the IR features near 2347 cm⁻¹ in dB15 is that they are all from CO₂. One interpretation is that the spectral structure comes from some CO₂ molecules being trapped solely by N₂ and others being surrounded by both H₂O and N₂, while another explanation is that CO₂ dimers or multimers are partly responsible. Within the astrochemical community, early work by Van der Zwet et al. (1989) found three CO₂ features in the 2347 cm⁻¹ region of the IR spectrum of N₂+CO₂ mixtures. Schriver et al. (2000) later reported that CO₂ that is matrix-isolated within N₂, even at high dilutions, exhibits multicomponent patterns in that same spectral region, with all IR peaks coming from one or more CO₂ molecules. Also, Zhang & Sander (2011) have reported multiple CO₂ positions near 2347 cm⁻¹ in N₂+CO₂+H₂O ices at 4.5 K, with N₂ as the matrix material. In short, without additional information the proposal of an IR feature of N₂ overlapping the ν_3 band of CO₂ in the spectrum of an N₂+H₂O ice must be rejected.

Appendix C

C.1. Reported Enrichment of ¹⁵N in Radiation-Chemical Products

Isotopic abundances are relevant to many astrochemical subfields, ranging from meteorites to planetary atmospheres to comets to the ISM. Isotope measurements can help reveal and

constrain evolutionary paths and physical conditions. Therefore, laboratory work that reveals pathways for altering isotopic ratios is of much interest.

Along these lines, the ice experiments of dB15 began with an N₂ ice matrix that had, apparently, a normal ¹⁴N-to-¹⁵N ratio of ~250 based on terrestrial nitrogen isotopic abundances. However, in the authors' Figures 7(a) and (b) and the accompanying text several IR peaks are assigned to ¹⁵N₃, ¹⁵N¹⁴N, and ¹⁵N¹⁴N₂. It is surprising that the IR bands of these ¹⁵N-azide radiation products are comparable to or larger than those from the expected ¹⁴N₃. Since the natural abundance of ¹⁵N is only about 0.4%, this assignment suggests that the experiments produced a stunning ¹⁵N isotopic enrichment for N₃ and that the enrichment did not extend to other radiation products, such as NO and NO₂. It is unclear why radiolysis should produce any such large ¹⁵N enrichment, much less one that is specific to a single product. Our own study of N₃ formation gave no detectable ¹⁵N enrichment (Hudson & Moore 2002), and we know of none reported by others (e.g., Tian et al. 1988; Jamieson & Kaiser 2007; Wu et al. 2012).

The ¹⁵N enrichment just described rests on the soundness of the assignments of weak IR features to N₃. Although the text of dB15 says that "doublets of four isotopologues of the azide radical are clearly marked," the relevant figure labels only five of the eight expected peaks, with one of those at roughly the same position as NO₂ and another at the same position as a residual peak of the unirradiated sample. Of the remaining three labeled peaks, their assignment to N₃ can be tested by seeing if slight increases in temperature cause them to disappear, due to thermal decay of the N₃ radicals. No such test was presented. We conclude that the ¹⁵N isotopic enrichment reported is not convincing, although N₃ is an expected radiolysis product.

ORCID iDs

Reggie L. Hudson  <https://orcid.org/0000-0003-0519-9429>

References

- Andraos, J. 1999, *JChEd*, **76**, 1578
 Arakawa, E. T., & Nielsen, A. H. 1958, *JMoSp*, **2**, 413
 Beckers, H., Willner, H., & Jacox, M. E. 2009, *Chem. Phys. Chem.*, **10**, 706
 Begun, G. M., & Fletcher, W. H. 1960, *JMoSp*, **4**, 388
 Bencivenni, L., Sanna, N., Schriver-Mazzuoli, A., & Schriver, A. 1996, *JChPh*, **104**, 7836
 Bennett, C. J., Chen, S., Sun, B., Chang, A. H. H., & Kaiser, R. I. 2007, *ApJ*, **660**, 1588
 Bennett, C. J., Pirim, C., & Orlando, T. M. 2013, *ChRv*, **113**, 9086
 Bernstein, M. P., & Sandford, S. A. 1999, *AcSpA*, **55**, 2455
 Boduch, P., Domaracka, A., Fulvio, D., et al. 2012, *A&A*, **544**, A30
 Bordalo, V., da Silveira, E. F., Lv, X. Y., et al. 2013, *ApJ*, **774**, 105
 Capellos, C., & Bielski, B. H. J. 1972, *Kinetic Systems: Mathematical Description of Chemical Kinetics in Solution* (New York: Wiley)
 Cocke, D. L., Gomes, J. A. G., Gossage, J. L., et al. 2004, *ApSpe*, **58**, 528
 Cruikshank, D. P., Brown, R. H., & Clark, R. N. 1984, *Icar*, **58**, 293
 de Barros, A. L. F., da Silveira, E. F., Bergantini, A., Rothard, H., & Boduch, P. 2015, *ApJ*, **810**, 156
 DeMore, W. B., & Davidson, N. 1959, *JChS*, **81**, 5869
 Dyke, J. M., Jonathan, N. B. H., Lewis, A. E., & Morris, A. 1982, *MolPh*, **47**, 1231
 Ehrenfreund, P., Boogert, A., Gerakines, P., & Tielens, A. 1998, *FaDi*, **109**, 463
 Ehrenfreund, P., Gerakines, P. A., Schutte, W. A., van Hemert, M. C., & van Dishoeck 1996, *A&A*, **312**, 263
 Forney, D., Thompson, W. E., & Jacox, M. E. 1993, *JChPh*, **99**, 7393
 Fredin, L., Neland, B., & Ribbegard, G. 1974, *JMoSp*, **53**, 410
 Grundy, W. M., Binzel, R. P., Buratti, B. J., et al. 2016, *Sci*, **351**, aad9189
 Hadjiivanov, K., & Knözinger, H. 1999, *Catalyst. Letters*, **59**, 21
 Hagen, W., Tielens, A. G. G. M., & Greenberg, J. M. 1981, *CP*, **56**, 567

- Halfen, D. T., Apponi, A. J., & Ziurys, L. M. 2001, *ApJ*, **561**, 244
- Harcourt, A. V., & Esson, W. 1866, *Phil. Trans.*, 156, 193
- Hartecck, P., & Dondes, S. 1958, *JChPh*, **28**, 975
- Hudgins, D. M., Sandford, S. A., Allamandola, L. J., & Tielens, A. G. G. M. 1993, *ApJS*, **86**, 713
- Hudson, R. L., Ferrante, R. F., & Moore, M. H. 2014, *Icar*, **228**, 276
- Hudson, R. L., Loeffler, M. J., & Gerakines, P. A. 2017a, *JChPh*, **146**, 0243304
- Hudson, R. L., Loeffler, M. J., & Yocum, K. M. 2017b, *ApJ*, **835**, 225
- Hudson, R. L., & Moore, M. H. 1997, *Icar*, **126**, 233
- Hudson, R. L., & Moore, M. H. 1999, *Icar*, **140**, 451
- Hudson, R. L., & Moore, M. H. 2002, *ApJ*, **568**, 1095
- Hudson, R. L., & Moore, M. H. 2004, *Icar*, **172**, 466
- Hudson, R. L., & Moore, M. H. 2018, *ApJ*, **857**, 89
- Hudson, R. L., Moore, M. H., & Gerakines, P. A. 2001, *JGRE*, **106**, 33275
- Hudson, R. L., Palumbo, M. E., Strazzulla, G., et al. 2008, in *The Solar System beyond Neptune*, ed. M. A. Barucci et al. (Tucson, AZ: Univ. Arizona Press), 507
- Ioppolo, S., Fedoseev, G., Minnisale, M., et al. 2014, *PCCP*, **16**, 8270
- Jamieson, C. S., Bennett, C. J., Mebel, A. M., & Kaiser, R. I. 2005, *ApJ*, **624**, 436
- Jamieson, C. S., & Kaiser, R. I. 2007, *CPL*, **440**, 98
- Jones, A. R. 1959, *RadR*, **10**, 655
- Koch, T. G., Horn, A. B., Chesters, M. A., McCoustra, M. R. S., & Sodeau, J. R. 1995, *JPhCh*, **99**, 8362
- Krim, L. 1998, *JMoSt*, **471**, 267
- Lapinski, A., Spanget-Larsen, J., Waluk, J., & Radziszewski, J. G. 2001, *JChPh*, **115**, 1757
- Lind, S. C., & Bardwell, D. C. 1929, *JACS*, **58**, 2751
- Loeffler, M. J., Teolis, B. D., & Baragiola, R. A. 2006, *JChPh*, **124**, 104702
- Louis, R. V., St., & Crawford, B., Jr. 1965, *JChPh*, **42**, 857
- Lovas, F. J., Hollis, J. M., Remijan, A. J., & Jewell, P. R. 2006, *ApJL*, **645**, L137
- McGuire, B. A., Carroll, P. B., Loomis, R. A., et al. 2016, *Sci*, **352**, 1449
- Mencos, A., Nourry, S., & Krim, L. 2017, *MNRAS*, **467**, 2150
- Minissale, M., Fedoseev, G., Congiu, E., et al. 2014, *PCCP*, **16**, 8257
- Moore, M. H. 1999, *Solid Interstellar Matter: The ISO Revolution* (Berlin: Springer)
- Moore, M. H., & Hudson, R. L. 2003, *Icar*, **161**, 486
- Moore, M. H., & Hudson, R. L. 2005, in *Proc. IAU Symp. 231, Production of Complex Molecules in Astrophysical Ices in Astrochemistry: Recent Successes and Current Challenges* (Cambridge Univ. Press), 247
- Moore, M. H., Hudson, R. L., & Gerakines, P. A. 2001, *AcSpA*, **57**, 843
- Mozumder, A. 1999, *Fundamentals of Radiation Chemistry* (San Diego, CA: Academic)
- Owen, T. C., Roush, T. L., Cruikshank, D. P., et al. 1993, *Sci*, **261**, 745
- Rodiguin, N. M., & Rodiguina, E. N. 1964, *Consecutive Chemical Reactions: Mathematical Analysis and Development* (Toronto: Van Nostrand)
- Rosu-Finsen, A., Marchione, D., Salter, T. L., et al. 2016, *PCCP*, **18**, 31930
- Rowland, B., Fisher, M., & Devlin, J. P. 1991, *JChPh*, **95**, 1378
- Sambrook, T. E. M., & Freeman, G. R. 1974, *JPhCh*, **78**, 28
- Sandford, S. A., Bernstein, M. P., Allamandola, L. J., Goorvitch, D., & Teixeira, T. C. V. 2001, *ApJ*, **548**, 836
- Satorre, M. Á., Domingo, M., Millan, C., et al. 2008, *P&SS*, **56**, 1748
- Savchenko, E. V., Khyzhniy, I. V., Uytunov, S. A., et al. 2014, *JPhChA*, **119**, 2475
- Schrifer, A., Schrifer-Mazzuoli, L., & Vigin, A. A. 2000, *Vibr. Spec.*, **23**, 83
- Secroun, C., Barbe, A., Jouve, P., Arcas, P., & Arie, E. 1981, *JMoSp*, **85**, 8
- Sicilia, D., Ioppolo, S., Vindigni, T., Baratta, G. A., & Palumbo, M. E. 2012, *A&A*, **543**, A155
- Smith, M. A. H., Rinsland, C. P., Fridovich, B., & Rao, K. N. 1985, in *Molecular Spectroscopy: Modern Research*, Vol. 3, ed. K. N. Rao (Orlando, FL: Academic), 111
- Soddy, F. 1911, *Ann. Rep. Chem. Soc.*, **8**, 269
- Stirling, A., Papai, I., Mink, J., & Salahub, D. 1994, *JChPh*, **100**, 2910
- Strazzulla, G. 1998, in *Solar System Ices*, ed. B. Schmitt, C. de Bergh, & M. Festou (Dordrecht: Kluwer), 281
- Swallow, A. J. 1973, *Radiation Chemistry* (New York: Wiley)
- Swanepoel, R. 1983, *JPhE*, **16**, 1214
- Tegler, S. C., Grundy, W. M., Olkin, C. B., et al. 2012, *ApJ*, **751**, 76
- Tempelmeyer, K. E., & Mills, D. W. 1968, *JAhPh*, **39**, 2968
- Terenishi, R., & Decius, J. C. 1954, *JChPh*, **22**, 896
- Thompson, W. E., & Jacox, M. E. 1990, *JChPh*, **93**, 3856
- Tian, R., Facelli, J. C., & Michl, J. 1988, *JPhCh*, **92**, 4073
- Tryka, K. A., Brown, R. H., & Anicich, V. 1995, *Icar*, **116**, 409
- Van der Zwet, G. P., Allamandola, L. J., Baas, F., & Greenberg, J. M. 1989, *JMoSt*, **195**, 213
- Van Thiel, M., Becker, E. D., & Pimentel, G. C. 1957, *JChPh*, **27**, 486
- Van Thiel, M., & Pimentel, G. C. 1960, *JChPh*, **32**, 133
- Varetti, E. L., & Pimentel, G. C. 1971, *JChPh*, **55**, 3813
- Varney, R. N. 1953, *PhRv*, **89**, 708
- Vasconcelos, F. A., Pilling, S., Rocha, W. R. M., Rothard, H., & Boduch, P. 2017, *PCCP*, **19**, 24154
- Williams, F. 1964, *JACS*, **86**, 3954
- Willis, C., & Boyd, A. W. 1976, *JRPC*, **8**, 71
- Willis, C., Boyd, A. W., & Young 1970, *CaJCh*, **48**, 1515
- Wourtsel, E. 1919, *Radium*, **11**, 289
- Wu, Y., Wu, C. Y. R., Chou, S., et al. 2012, *ApJ*, **746**, 175
- Yamada, H., & Person, W. B. 1964, *JChPh*, **41**, 2478
- Zhang, X., & Sander, S. P. 2011, *JPCA*, **115**, 9854
- Zheng, W., Jewitt, D., Osamura, Y., & Kaiser, R. I. 2008, *ApJ*, **674**, 1242
- Zheng, W., Kim, Y. S., & Kaiser, R. I. 2011, *PCCP*, **13**, 15749
- Zhun, I., Zhou, X., & Liu, R. 1996, *JChPh*, **105**, 11366
- Ziegler, J. F., Biersack, J. P., & Littmark, U. 1985, *The Stopping and Range of Ions in Solids* (New York: Pergamon), <http://www.srim.org/>
- Ziegler, J. F., & Manoyan, J. M. 1988, *NIMPB*, **35**, 218